

Chapter 11

Mesoporous Carbon for Energy

Pengfei Zhang and Sheng Dai

Abstract Ordered mesoporous carbons (OMCs) are of great interest in energy-related research and applications, partly due to their high surface areas, uniform pore channels, and narrow pore size distributions. During the past decades, a number of breakthroughs for the synthesis of OMCs, including hard templating methods and soft templating strategies, have been made by carbon chemists. Thanks to unique properties, OMCs-based supercapacitors are attracting more and more attention around the world in recent years in view of their ultrafast charge-discharge rate, high power capability, low maintenance, and long cycle life. In this chapter, we wish to overview those representative pathways for OMC materials and their performance in supercapacitor application.

11.1 Introduction

In the past decades, porous carbon materials have manifested themselves in various applications, such as: development of new electrical energy storage and conversion devices, catalyst or catalyst support, gas storage systems, etc. [1]. The importance of these carbonaceous materials actually resides in their excellent physical and chemical properties tunable in a wide range, such as high surface area, large pore volumes, good electronic conductivity, designable chemical composition, chemical and thermal stability [2, 3]. Nowadays, carbon materials with various pore structures (e.g. micropore, mesopore) have been devised by different synthetic strategies [4, 5]. Being the most popular and frequently used carbons, activated

P. Zhang · S. Dai
Chemical Sciences Division, Oak Ridge National Laboratory, Oak Ridge, TN 37831, USA

S. Dai (✉)
Department of Chemistry, University of Tennessee, Knoxville, TN 37996, USA
e-mail: dais@ornl.gov

carbons, dominated by micropores, are generally prepared from carbonization of biomass sources such as coconut, coal and further activations involving exposure in harsh oxidizing atmospheres (e.g. CO₂, steam) or chemical treatment with acids (e.g. phosphoric acid), bases (e.g. KOH, NaOH), or salts (e.g. ZnCl₂, SnCl₂) are necessary for directing porosity [6–8]. Meanwhile, carbon materials with well-defined mesopore have received significant attention owing to their large and tunable pore size and uniform pore channel, which would be beneficial to various fields, such as: carbon-based supercapacitor [9–11].

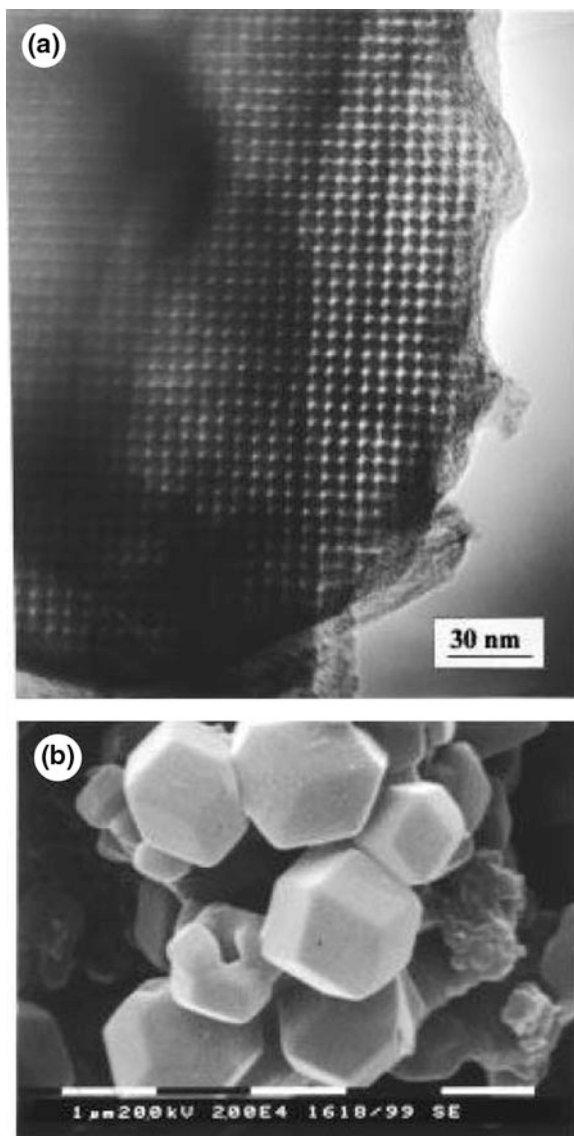
Nowadays, the fast growth of portable electronic devices and hybrid electric vehicles has promoted the urgent and increasing demand for high-power energy storages, such as supercapacitors. At present, activated carbons are widely used as the electric double layer capacitor (EDLC) electrode materials because of their low cost, scalable character and a variety of biomass precursors. Though conventionally activated carbons possess a large surface area, their EDLC performance can be somewhat limited because they actually contain an abundant proportion of micropores not always fully accessible to big ions [12, 13]. Therefore, only exposed outer surface are utilized for charge storage. In addition, even in the situation wherein the micropores are filled by the electrolyte, the ionic transfer in such small pores may be so slow that the high rate capability could not be reached. Both charge storage and rate capability are also limited by the randomly connected pores within activated carbon. In contrast, ordered mesoporous carbon materials at this stage could resolve above-mentioned questions for promising energy devices [14]. In this chapter, we wish to summarize recent advances on the preparation of ordered mesoporous carbons (OMCs) and their applications as supercapacitors. Ordered mesoporous carbons are generally fabricated by a hard or soft-templating approach, as shown in the following.

11.2 Ordered Mesoporous Carbons (OMCs) from Hard-Templating Method

Ryoo's groups for the first time introduced OMCs in 1999, where mesoporous MCM-48 derived from the surfactant self-assembly approach was used as the hard template and sucrose inside the pores of the MCM-48 was carbonized in N₂ [15]. The CMK-1 carbon was obtained after subsequent removal of the silica template with a hot ethanolic solution of NaOH (Fig. 11.1). X-ray powder diffraction (XRD) pattern of CMK-1 indicated the highly ordered pore arrangement and the CMK-1 carbon underwent a systematic transformation into new structural symmetry from that of the silica template. The nitrogen adsorption isotherm of CMK-1 featured a sharp adsorption step owing to the capillary condensation of N₂ molecules inside these uniform mesopores (Fig. 11.2).

Three months later, Hyeon et al. reported the synthesis of another OMC material by also employing mesoporous MCM-48 aluminosilicate with three-dimensional

Fig. 11.1 **a** Representative transmission electron micrograph of the ordered carbon molecular sieve CMK-1, obtained by the template synthesis with the mesoporous silica molecular sieve MCM-48. This image was obtained with a Philips CM20 transmission electron microscope operated at 100 kV from thin edges of a particle supported on porous carbon grid. **b** Scanning electron micrograph of a CMK-1 sample. This image was obtained on a Philips SEM-535M microscope using an acceleration voltage of 20.0 kV. Reproduced with permission from [15]. Copyright 1999 American Chemical Society



channel structure as the template and with phenolic resin as the carbon source [16]. The dissolution of MCM-48 frameworks using 48 % aqueous hydrofluoric acid generated mesoporous carbon, designated SNU-1. The specific surface area of SNU-1 was found to be 1257 m²/g from nitrogen BET adsorption measurements (Fig. 11.3). Nitrogen adsorption–desorption curves showed hysteresis at high relative pressure characteristic of mesopores. The pore size distribution data calculated from the adsorption branch of the nitrogen isotherm by the BJH (Barrett–Joyner–

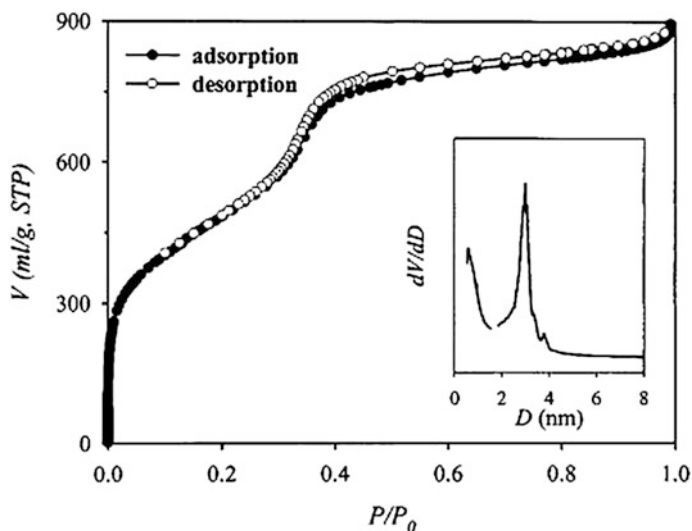


Fig. 11.2 Argon adsorption-desorption isotherms at 87 K for the carbon molecular sieve CMK-1. *Inset* The corresponding pore size distribution curves obtained from the desorption by the Barrett–Joyner–Halenda method (>1.7 nm), and the Horvath–Kawazoe analysis (0.5–1.7 nm). Reproduced with permission from [15]. Copyright 1999 American Chemical Society

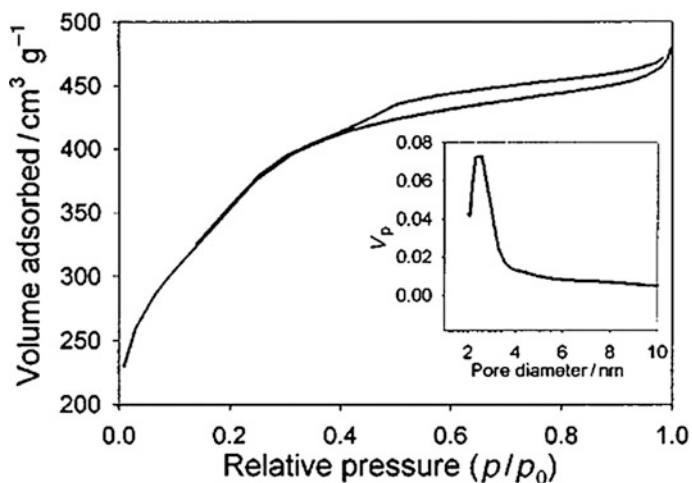


Fig. 11.3 N_2 adsorption and desorption isotherms of mesoporous SNU-1 carbon. *Inset* The corresponding pore size distribution curve calculated from the adsorption branch of the nitrogen isotherm by the BJH method. V_p is the incremental pore volume. The isotherms were collected at 77 K on a Micrometrics ASAP2010 Gas Adsorption Analyzer after the carbon material was degassed at 250 °C at 30 mTorr for 5 h. Reproduced with permission from [16]. Copyright 1999 Royal Society of Chemistry

Halenda) method showed that pores are uniform with an average pore size of 2.3 nm. The performance of SNU-1 in an electrochemical double-layer capacitor was also evaluated by the same group. In this topic, our group introduced the mesoporous carbon “C48” using mesophase pitch as the carbon precursor and MCM-48 silica as a hard template. The C48 material exhibited XRD patterns similar to that of CMK-1 [17, 18]. The framework of the C48 carbon network was composed of carbon nanorods of 1.5–2 nm length interconnected in three-dimensions.

Besides MCM-48, the hexagonally structured SBA-15 mesoporous silica (SBA-15) was another frequently-investigated hard template for OMC synthesis. For example, a highly ordered, hexagonal OMC-CMK-3, was reported by Ryoo and co-workers with SBA-15 as the template. CMK-3 is composed of carbon nanorods arranged in a hexagonal pattern, with connecting bridges between them (Fig. 11.4) [19]. Actually, the specific surface area of CMK-3 was higher than calculated value for CMK-3 with nonporous pore wall, suggesting that pore wall of CMK-3 was rich in complementary micropores (Fig. 11.5). The pore size of OMC material synthesized with a hard template is primarily controlled by the pore wall thickness of the inorganic templates, which can be in principle tailored by the selection of template.

In addition, various carbon precursors, e.g., sucrose, furfuryl alcohol, naphthalene, C_2H_2 , polyacrylonitrile, and phenolic resin, can be utilized for OMCs. For example, Schüth and Lu reported nitrogen-containing OMC with well-developed bimodal system by using SBA-15 as template and polyacrylonitrile as carbon source via a nanocasting pathway (Fig. 11.6) [20, 21]. However, those hard templating methods require the preparation of mesoporous silica, adding time and

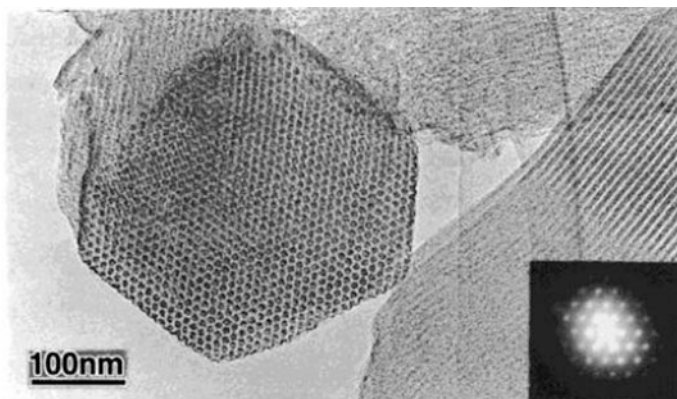
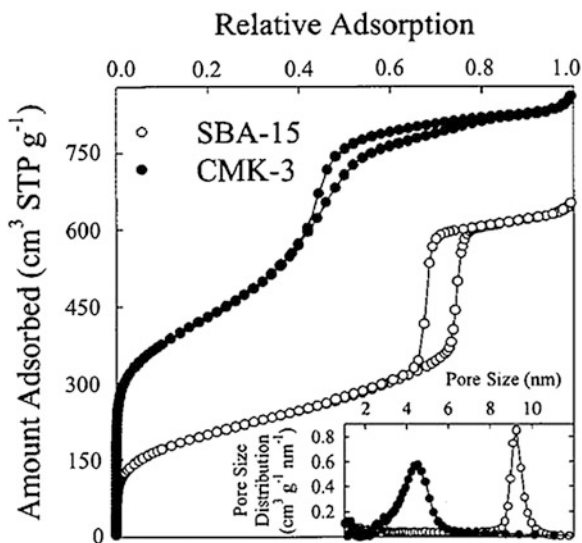


Fig. 11.4 Typical TEM images of the ordered mesoporous carbon molecular sieve, CMK-3. This carbon was synthesized using sucrose as a carbon source and SBA-15 silica as a template. The TEM images were obtained with a JEM-4000 EX operated at 400 kV from the carbon material after silica template was completely removed with HF solution. Reproduced with permission from [19]. Copyright 2000 American Chemical Society

Fig. 11.5 N₂ adsorption–desorption isotherm at 77 K for CMK-3 and SBA-15. *Inset* The pore size distributions. Reproduced with permission from [19]. Copyright 2000 American Chemical Society



increased costs to the preparation of the final carbon materials and the use of concentrated sodium hydroxide or toxic hydrofluoric acid for removing templates makes this process difficult in industrial scale. Complementary to the hard-templating method, the soft-templating synthesis of mesoporous carbons by the organic–organic self-assembly offers several advantages in terms of cost and processing possibility [22].

11.3 Ordered Mesoporous Carbons from Soft-Templating Method

Somewhat like the self-assembly process for ordered mesoporous metal oxides developed earlier [23], soft templating construction of OMCs relies on the cooperative assembly between structure-directing templates and organic carbon sources during initial polymerization. In 2004, our group for the first time showed the synthesis of ordered mesoporous carbon films by a soft template route [24]. This methodology involves pre-organization of the resorcinol monomers and polystyrene-block poly(4-vinylpyridine) (PS-P4VP) into a nanostructured film with hydrogen bond induced self-assembly (Fig. 11.7). Formaldehyde gas was then vaporized to the film for in situ cross-linking the resorcinol monomers. The resulting resorcinol-formaldehyde resin was transformed into a highly ordered mesoporous carbon film during carbonization process, while those PS-P4VP template decomposed into gaseous species. SEM and TEM images illustrated that the pore diameter is 33.7 ± 2.5 nm and the wall thickness is 9.0 ± 1.1 nm (Fig. 11.8). This soft-templating approach actually inspired rapid progresses in this topic.

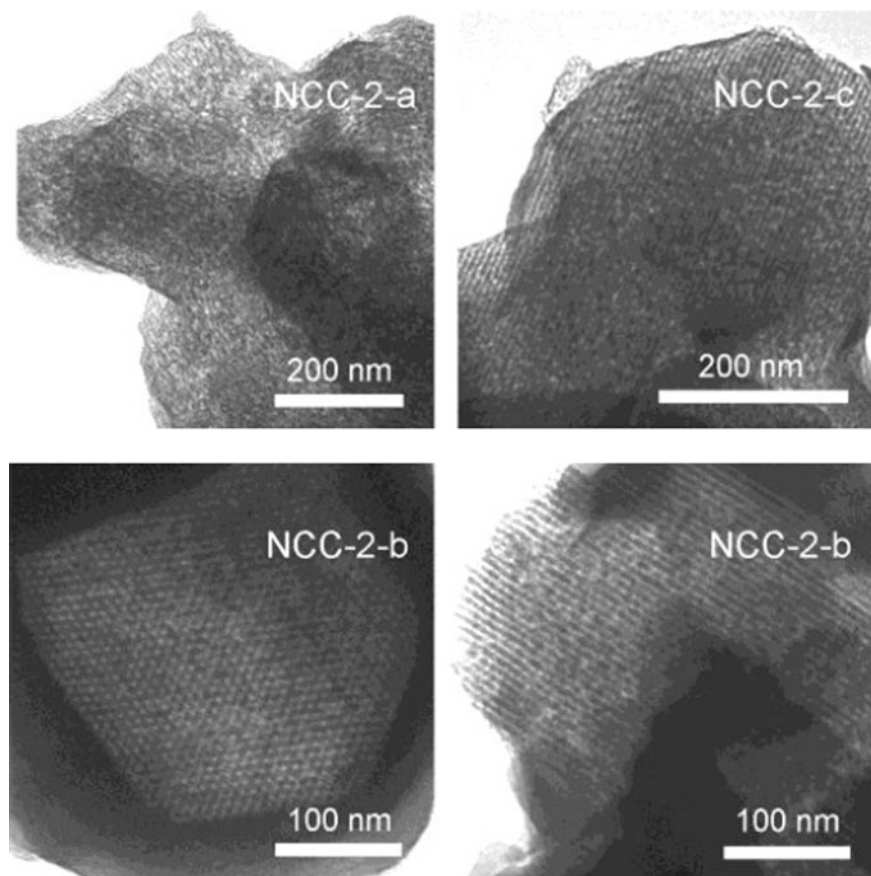


Fig. 11.6 TEM images of NCC-2-a, NCC-2-b, and NCC-2-c. Reproduced with permission from [21]. Copyright 2004 American Chemical Society

In addition to PS-P4VP, other block copolymers were also developed as soft templates for OMCs. Tanaka and co-workers showed the possibility of common Pluronic PEO-*b*-PPO-*b*-PEO as soft template. They carried out the resorcinol-formaldehyde polymerization in the presence of Pluronic F127 and triethyl orthoacetate as co-precursor (Fig. 11.9) [25]. The co-precursor triethyl orthoacetate here increased the ordering of the porous structure in some degree. Zhao's group completed a detailed investigation of OMCs prepared with different co-polymers, such as F127, F108 and P123 [26–28]. For example, the pore morphology of as-made OMCs could be controlled by the fraction of the hydrophobic block during polymerization, that is tuning the PEO content in the copolymer or changing the ratio of carbon precursor-to-template (Fig. 11.10). Different mesostructures of OMCs, including lamellar (La), bicontinuous (Ia3d), hexagonal (p6mm) and cubic globular (Im3m) could be obtained by increasing curvature at the micelle interface.

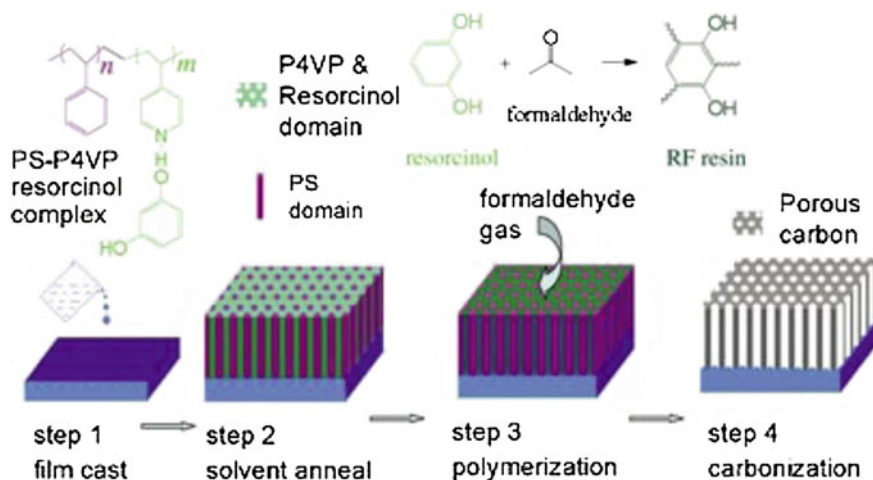


Fig. 11.7 Schematic representation of the synthesis protocol used to prepare well-defined carbon nanostructures. *Step 1* Film casting of PS-P4VP/resorcinol supramolecular assembly. *Step 2* Completion of microphase separation by solvent annealing at 80 °C in DMF/benzene mixed vapor. The resorcinol is organized in the well-defined P4VP domain. *Step 3* In situ polymerization of resorcinol and formaldehyde by exposing the film to formaldehyde gas. Highly cross-linked RFR is formed within the P4VP domain. *Step 4* Pyrolysis of the polymeric film in N₂. A hexagonal carbon-channel array is formed by sacrificing the block copolymer. Reproduced with permission from [24]. Copyright 2004 Wiley-VCH Verlag GmbH & Co. KGaA, Weinheim

Just recently, our group established a surfactant-free synthesis of mesoporous carbon materials through the polymerization of phloroglucinol-formaldehyde resins in the presence of polyethylene glycol (PEG) with acidic ethanol (Fig. 11.11) [29]. The essence of this strategy relies in the PEG-mediated spinodal decomposition for porosity control, instead of the traditional micellar self-assembly approaches. Mesoporous carbons with specific surface areas up to 392 m²/g and pore size around 20 nm could be fabricated by this method (Fig. 11.12). In comparison with those triblock copolymers, utilization of linear PEG as a sacrificial soft-template provides a more sustainable alternative for OMCs.

In the past decade, a family of carbon precursors, such as phenol, resorcinol and phloroglucinol, were employed for the synthesis of soft-templated OMCs, most of which were based on chemistry of phenol-aldehyde polymerization. Those molecules forms hydrogen-bonded networks with block polymers and then are cross-linked by formaldehyde in the presence of acid or base catalyst. The hydroxy group on the substrate is a key point for interacting with soft template. For example, Dai and co-workers studied the polymerization processes by phenol-formaldehyde, resorcinol-formaldehyde and phloroglucinol-formaldehyde [30]. It was observed that phloroglucinol could complete the polymerization more rapid than resorcinol or phenol (40 min vs. 1–3 weeks, respectively). The authors considered that the high hydroxy density in the oligomers formed from phloroglucinol provides a greater

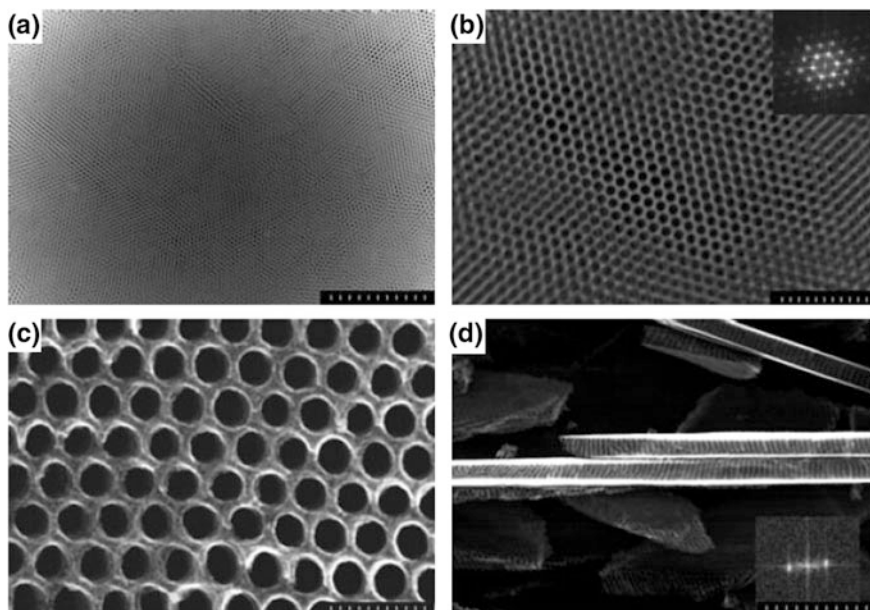


Fig. 11.8 Electron microscopy images of the carbon film. **a** Z-contrast image of the large-scale homogeneous carbon film in a $4 \times 3 \mu\text{m}$ area. The scale bar is $1 \mu\text{m}$. **b** Z-contrast image showing details of the highly ordered carbon structure. In the *inset*, a Fourier transform (FT) of the image shows a pattern with multiple reflections, which are characteristic of a highly ordered hexagonal array. The scale bar is 300 nm . **c** High-resolution SEM image of the surface of the carbon film with uniform hexagonal-pore array. The pore size is $33.7 \pm 2.5 \text{ nm}$ and the wall thickness is $9.0 \pm 1.1 \text{ nm}$. The scale bar is 100 nm . **d** SEM image of the film cross section, which exhibits all parallel straight channels perpendicular to the film surface. The scale bar is 100 nm . The inset is the FT of the cross section image. The FT pattern shows the reflections of the periodic parallel channels. Reproduced with permission from [24]. Copyright 2004 Wiley-VCH Verlag GmbH & Co. KGaA, Weinheim

driving force for the self-assembly interaction with the PEO blocks, as compared with those provided by the oligomers from phenol and resorcinol (Fig. 11.13).

Considering environment and sustainability issues, above methods with fossil-based sources are restricted for long term development. It seems of great interest to develop renewable carbon sources for the synthesis of OMCs. Antonietti and co-workers recently illustrated another OMCs by hydrothermal carbonization (HTC) of fructose in the presence of block copolymer surfactant Pluronic F127 [31]. Since HTC of fructose can occur under relatively low temperature (e.g. $130 \text{ }^\circ\text{C}$), fructose was selected for this micellar self-assembly. HTC of fructose with F127 additive can lead to composite material, presenting a well ordered structure with an F127 micelle diameter of $\sim 10 \text{ nm}$ and carbon wall thickness of $\sim 6 \text{ nm}$ (Fig. 11.14). Though corresponding carbon material after thermal treatment ($550 \text{ }^\circ\text{C}$) showed long-range regularly ordered pore structure with cubic $\text{Im}3\text{m}$ symmetry (From HRTEM and SSAXS analysis), N_2 sorption analysis presented a non-reversible microporous type I

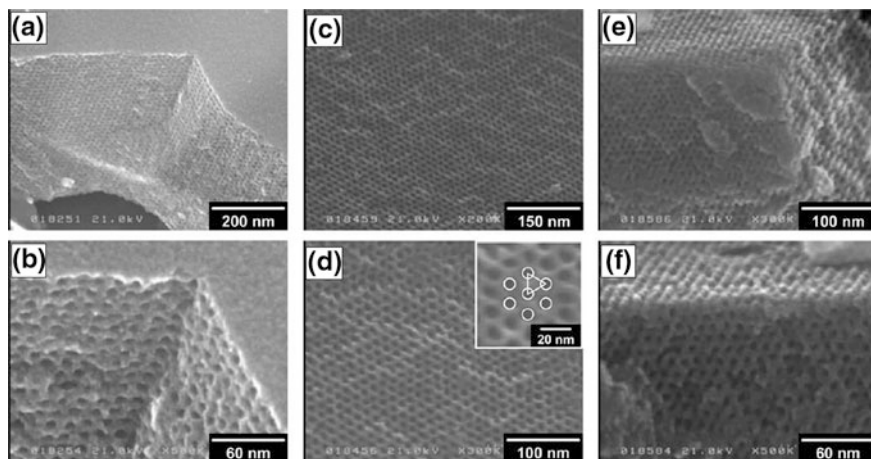


Fig. 11.9 FE-SEM images of carbonized COU-1. The carbonization temperatures were as follows: **a, b** 400 °C, **c, d** 600 °C and **e, f** 800 °C. Reproduced with permission from [25]. Copyright The Royal Society of Chemistry 2005

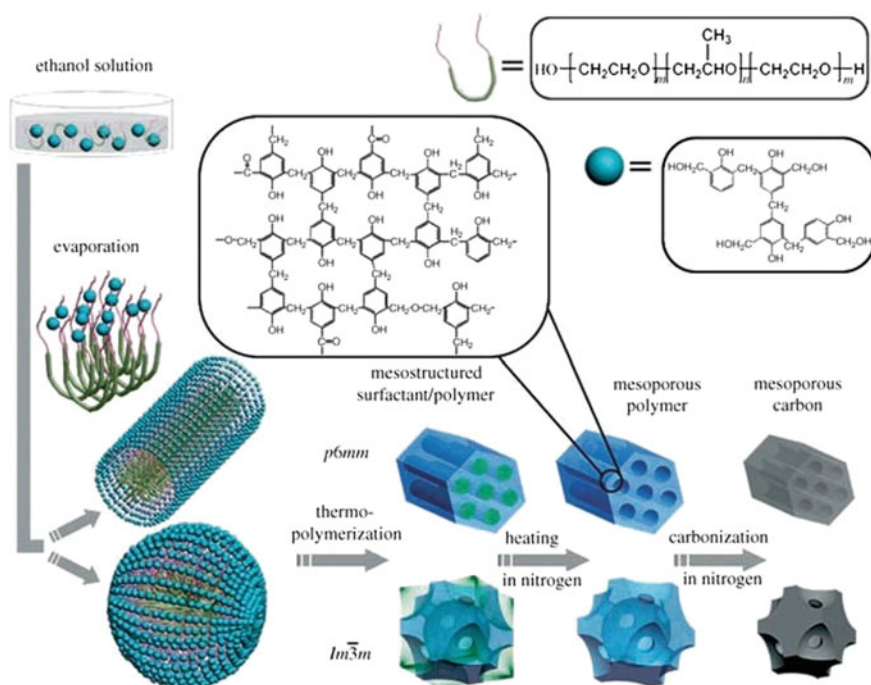


Fig. 11.10 Schematic representation of the procedure used to prepare mesoporous carbon frameworks. Reproduced with permission from [27]. Copyright 2005 Wiley-VCH Verlag GmbH & Co. KGaA, Weinheim

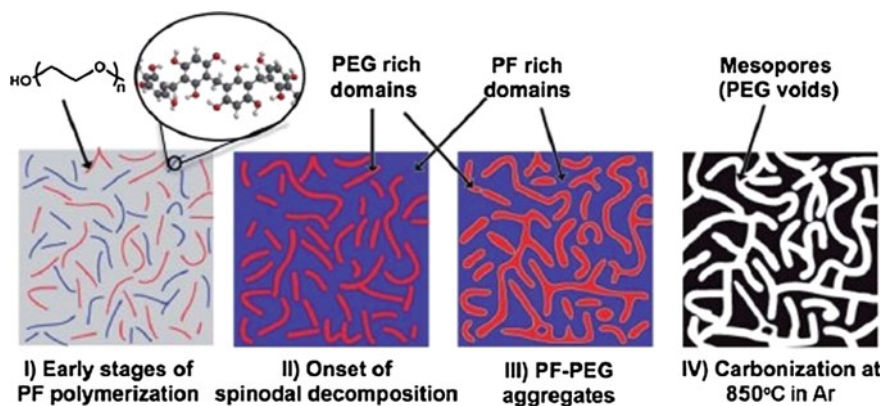


Fig. 11.11 Schematic illustration of spinodal decomposition (I–III) and subsequent formation of mesoporous carbon (IV) from PF–PEG adduct. Reproduced with permission from [29]. Copyright The Royal Society of Chemistry 2014

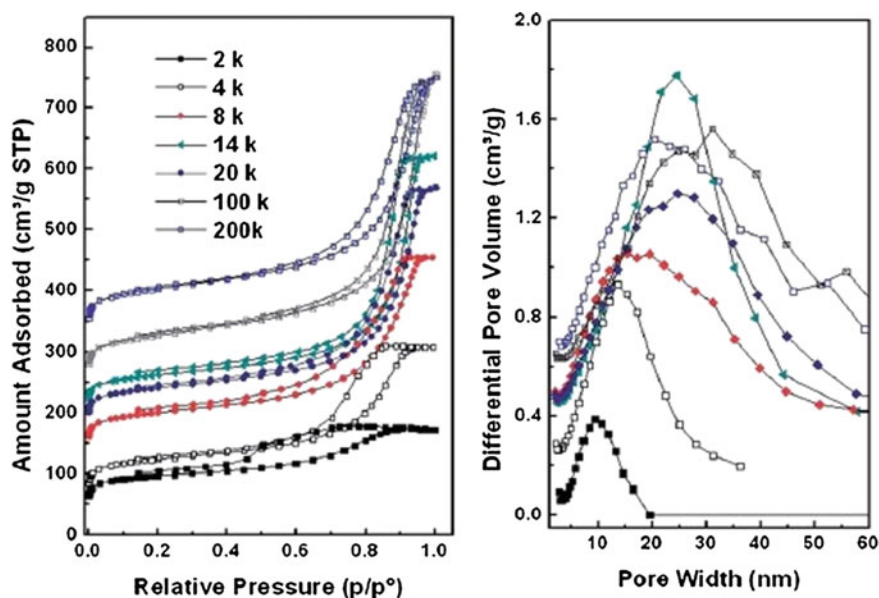


Fig. 11.12 Nitrogen $-196\text{ }^{\circ}\text{C}$ adsorption isotherms (*left*) and corresponding pore size distributions (*right*) calculated using KJS method of carbon samples with respective PEG (in Da). For clarity, the isotherms were offset by consecutive increments of $50\text{ cm}^3/\text{g}$ and pore size distributions offset in consecutive increments of $0.2\text{ cm}^3/\text{g}$. Reproduced with permission from [29]. Copyright The Royal Society of Chemistry 2014

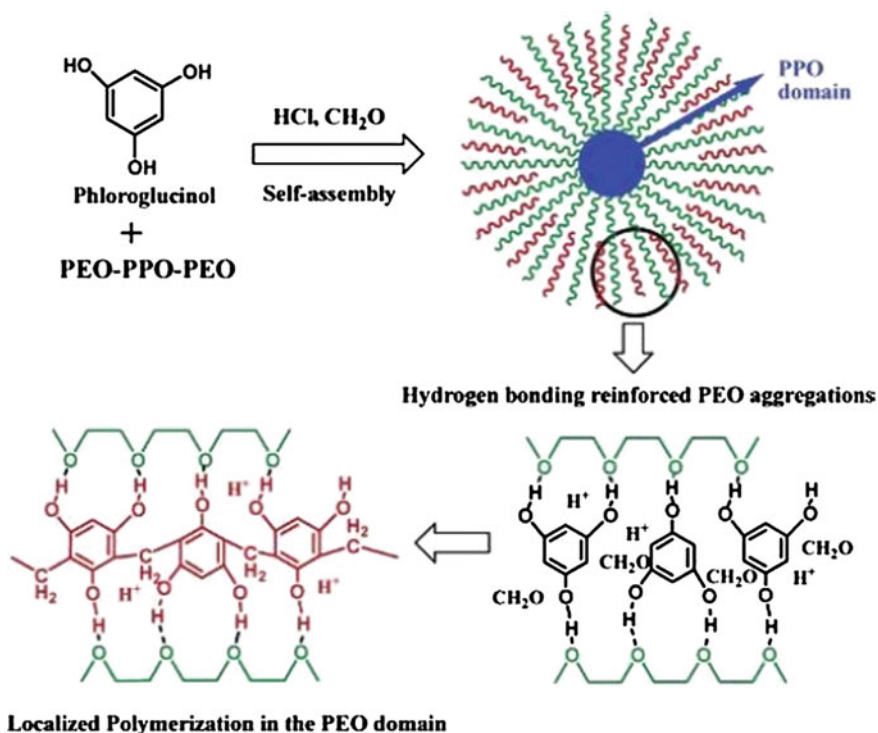


Fig. 11.13 Localized Polymerization. Reproduced with permission from [30]. Copyright 2006 American Chemical Society

isotherm with pore size distribution around 0.9 nm (Fig. 11.15). The authors attribute the narrowed pores during template removal to structural shrinkage or partial co-carbonization of the block copolymer inside channels. To shift pore structure into the mesoporous domain, the swelling agent trimethylbenzene was added to the F127/ Fructose mixture for larger micelles. OMC material with a type IV N_2 sorption profile and capillary condensation feature at $P/P_0 \approx 0.45$, was observed and the BET surface area is $116 \text{ m}^2/\text{g}$, giving another pathway for OMC family (Fig. 11.16). During suggested mechanism for this process, fructose is absorbed in the initial stages via H-bonding with the hydrophilic PEO moiety of F127 (or with TMB additive) and then proceeds dehydration/polycondensation to generate a polyfuran-like network for further thermal treatment ($550 \text{ }^\circ\text{C}$).

Another biomass product—tannin with multi phenolic hydroxyls were just recently explored for the synthesis of OMCs. Parmentier and co-workers synthesized OMC materials with tannin extracted from wattle barks as carbon source via the self-assembly process of an amphiphilic triblock copolymer [32]. Tannins are naturally present in plants and have well known and established processes for their extraction from wood materials. Tannins on their own are also able to self-condense

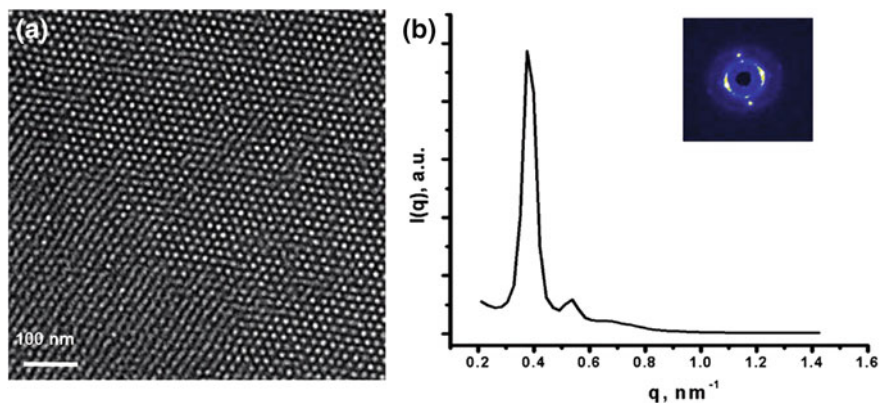


Fig. 11.14 **a** TEM micrograph and **b** Synchrotron SAXS pattern of C-MPG1-com (inset 2D scattering pattern). Reproduced with permission from [31]. Copyright 2011 American Chemical Society

to form a three-dimensional network by creating covalent bonds between the different flavonoid units and no cross-linker agents were needed in this process. In this process, the multiple adjacent hydroxyl groups of flavonoid unit probably play a key role for the self-assembly with PEO via hydrogen bonds (Fig. 11.17). OMC materials with specific surface area up to $545 \text{ m}^2/\text{g}$ and pore size around 7–9 nm were obtained (Fig. 11.18). This tannin-based approach with cheap, renewable and non toxic precursor provides a greener way for OMC materials.

Recently, Wang and co-workers reported a self-transformation strategy to control the Fructose based HTC/soft templating. Insoluble melamine sulphates were introduced to direct the HTC/F127 procedure [33]. During this process, melamine sulphates were co-assembled and copolymerized with fructose, and further in situ transformed into OMC products with N-doping. HRTEM images exhibited ordered pores in the carbon flakes with pore diameter around 3 nm and wall thickness about 10 nm. The N_2 sorption analysis ($S_{\text{BET}} = 761 \text{ m}^2/\text{g}$) presented a type IV isotherm and the pore size distribution showed a sharp peak at 3.3 nm and a broad shoulder less than 2 nm (Fig. 11.19).

11.4 Ordered Mesoporous Carbons for Supercapacitor

Hyeon and co-worker studied the EDLC performance of SNU-1 sample in 1999 [16]. Comparing with activated carbon, MSC-25, the SNU-1 sample showed a more ideal capacitor behavior with a more rectangular-shaped cyclic voltammogram (CV) curve. When the scan rates were enhanced from 5 to 50 mV s^{-1} , SNU-1 carbon retained a rectangular shape up to a scan rate of 20 mV s^{-1} . By contrast, MSC-25 carbon showed a deformed CV curve at a scan rate of 10 mV s^{-1} and a

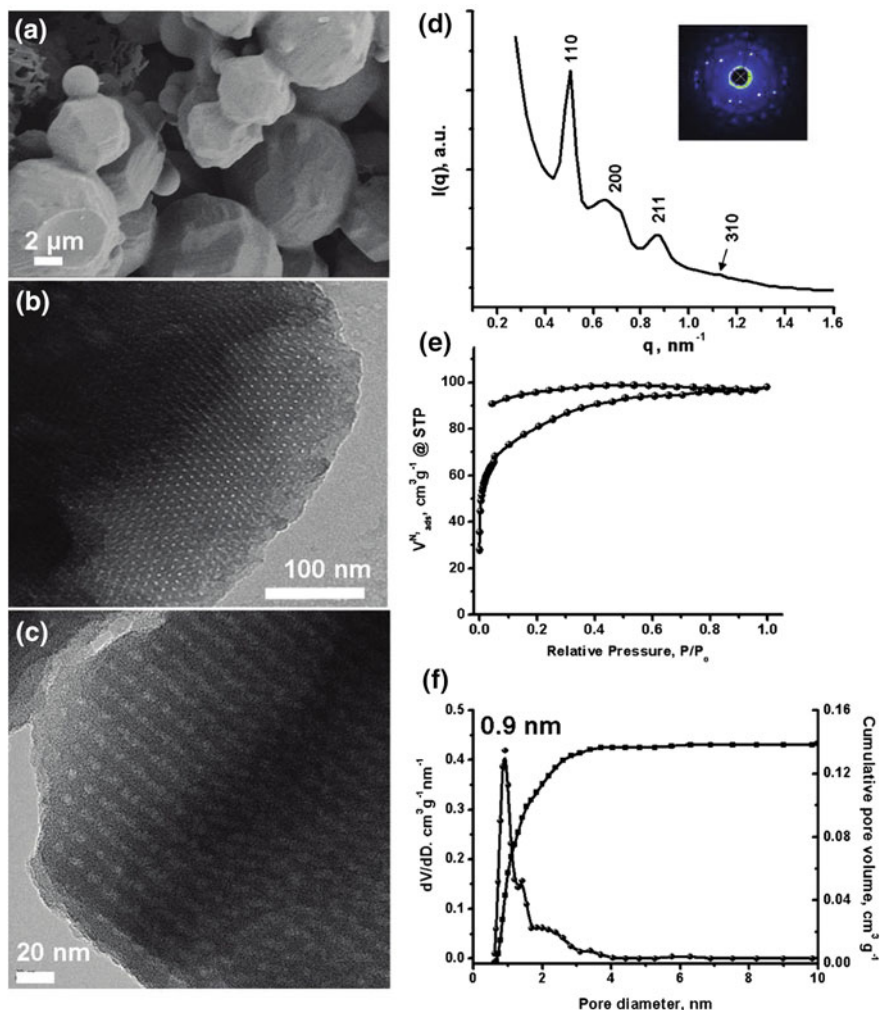


Fig. 11.15 a SEM, b TEM, c HRTEM micrographs, d synchrotron SAXS pattern (*inset* 2D scattering pattern), e N_2 sorption isotherm, and f QSDFT pore size distribution of C-MPG1-*micro*. Reproduced with permission from [31]. Copyright 2011 American Chemical Society

completely collapsed one at a scan rate of 20 mV s^{-1} (Fig. 11.20). Those results reflected the advantage of regular interconnected mesopores for fast electrolyte transfer.

Specific surface areas of OMC materials are generally considered as key factors for the EDLC performance, since EDLCs utilize the electric double layer formed at the electrode/electrolyte interface for charge storage. An activation process by heating a physical mixture of potassium hydroxide and soft-template OMC within

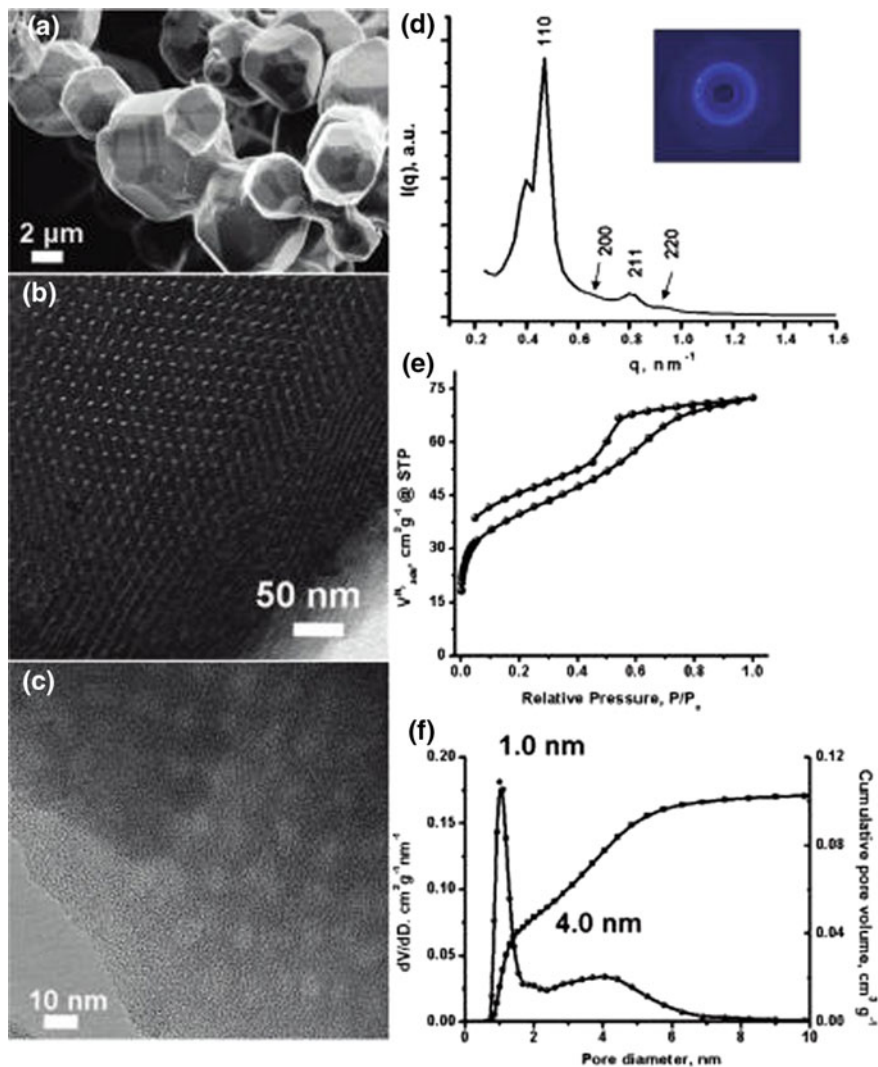


Fig. 11.16 a SEM, b TEM, and c HRTEM micrographs, d synchrotron SAXS pattern (inset 2D scattering pattern), e N₂ sorption isotherm, and f QSDFT pore size distribution of as-synthesized C-MPG1-*meso*. Reproduced with permission from [31]. Copyright 2011 American Chemical Society

N₂ at high temperatures (400–1000 °C), was introduced for higher surface areas [34]. The quantity of KOH and activation temperature affected the activation process, and the increased surface area was induced by activation-developed micropore. Around 70 % of the total surface area came from micropore. In addition, this activation process would increase carbon burn-off with lower carbon yield. Being as

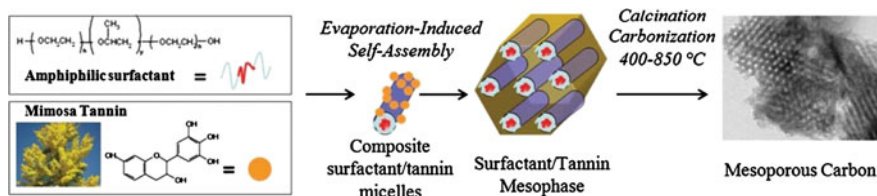


Fig. 11.17 Scheme for the synthesis of the ordered mesoporous polymer and carbon materials. Reproduced with permission from [32]. Copyright The Royal Society of Chemistry 2012

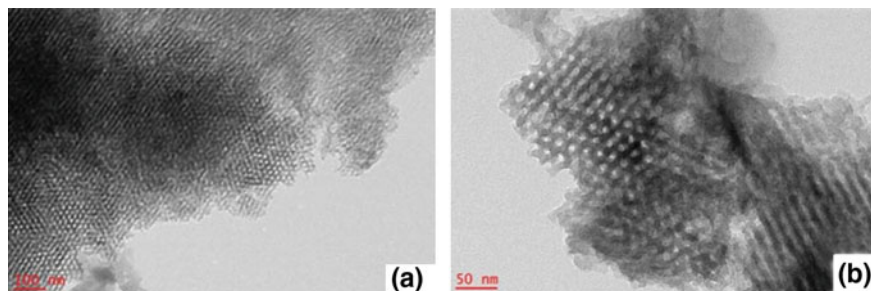


Fig. 11.18 TEM micrographs of the IS2M-1 phase (tannin-derived polymer) obtained by the evaporation self-assembly process and calcined at 400 °C. The low magnification (a) shows the limited size of the ordered domains (b). Reproduced with permission from [32]. Copyright The Royal Society of Chemistry 2012

EDLCs, activated OMC with surface area of 1940 m²/g showed a specific capacitance of 188 F/g at a sweep scan rate of 1 mV/s in 0.1 M sodium chloride aqueous electrolyte, much higher than the capacitance (71.3 F/g) by only OMC sample from phenolic resin precursors (520 m²/g). Liu and co-workers illustrated a silica-assisted co-assembly route to OMCs. In their strategy, the mixture of phenol-formaldehyde resol and tetraethyl orthosilicate were used to co-assembly in the presence of F127 by an EISA strategy. After triblock polymer removal, carbonization and HF acid etching of silica, OMC with pore size around 6.7 nm and extremely high surface area could be obtained [35]. When this sample was studied as EDLC electrode within organic electrolyte [(C₂H₅)₄N][BF₄], a good capacitance of 112 F/g between 0 and 3 V was observed at a scan rate of 200 mV/s. Importantly, an outstanding stability with capacitance retention of 88 % was got by this sample after 1000 cycles [36].

In addition, increasing efforts have been recently devoted to the synthesis of element-doped mesoporous carbons, which could combine the high mesoporosity and unique characters of doped carbon frameworks, such as: enhanced mechanical, semiconducting, field-emission and electrical properties. Zhao and co-workers reported nitrogen-doped OMC material with a high N content by using evaporation-induced self-assembly of a low-molecular-weight soluble resol and dicyandiamide

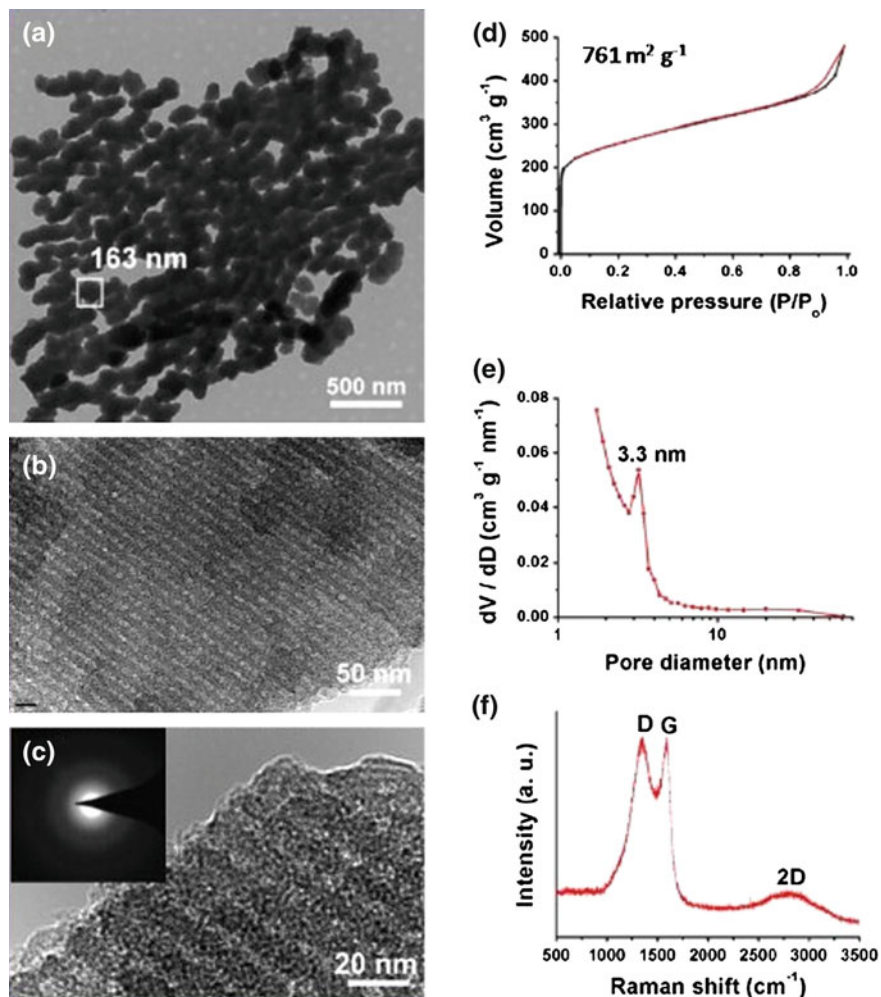


Fig. 11.19 Characterizations of sample OMCC-3-1 prepared at a DFructose/melamine molar ratio of 3 and a sulphuric acid/melamine molar ratio of 1: **a** TEM image; **b** and **c** HRTEM micrographs (*inset* the 2D scattering pattern); **d** N₂ sorption isotherm; **e** pore size distribution curve; **f** Raman spectra. Reproduced with permission from [33]. Copyright 2014 American Chemical Society

in the presence of F127 template (Fig. 11.21) [3]. The high nitrogen content (up to 13.1 %) was attributed to the introduction of DCDA, since it could form stable microdomains of carbon nitrides in the matrix of phenolic resin. The nitrogen-doped OMC sample exhibited good performance as supercapacitor electrodes, with specific capacitance of 262 F/g (1 M H₂SO₄) and 227 F/g (6 M KOH) at a current density of 0.2 A/g, better than that by the mesoporous FDU-15 carbon without nitrogen modification (Fig. 11.22).

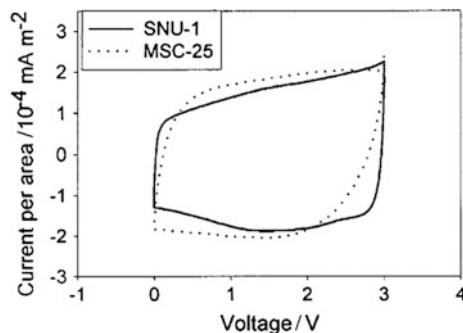


Fig. 11.20 Cyclic voltammograms of SNU-1 and MSC-25 activated carbon in organic electrolyte (1 M NEt_4BF_4 in propylene carbonate). A two-electrode system consisting of working and counter electrodes was used. These two electrodes were fabricated with equal amounts of the carbon materials. CV measurements were made in the potential range 0–3 V with a scan rate of 5 mV/s. Reproduced with permission from [16]. Copyright 1999 Royal Society of Chemistry

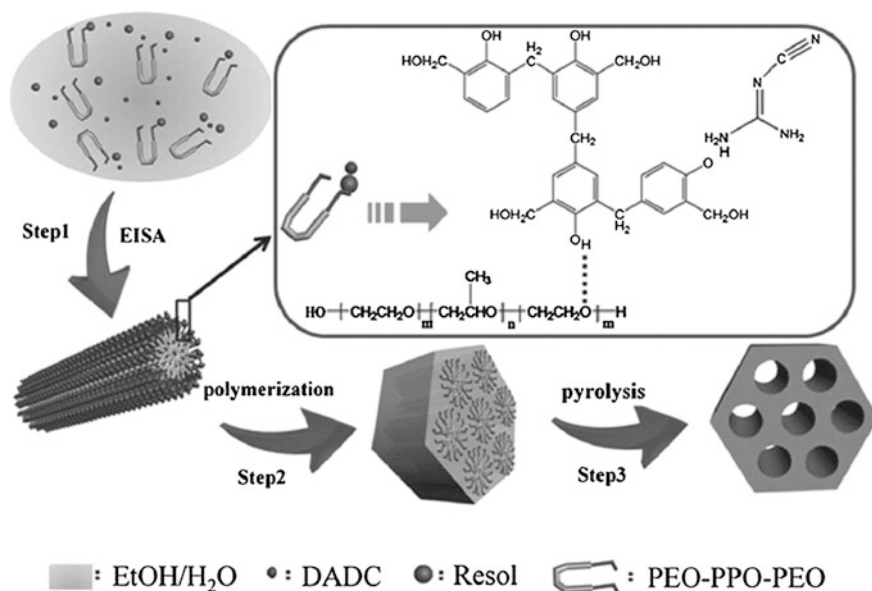


Fig. 11.21 The formation process of ordered N-doped mesoporous carbon from a one-pot assembly method using dicyandiamide (DCDA) as a nitrogen source. Reproduced with permission from [3]. Copyright 2013 Wiley-VCH Verlag GmbH & Co. KGaA, Weinheim

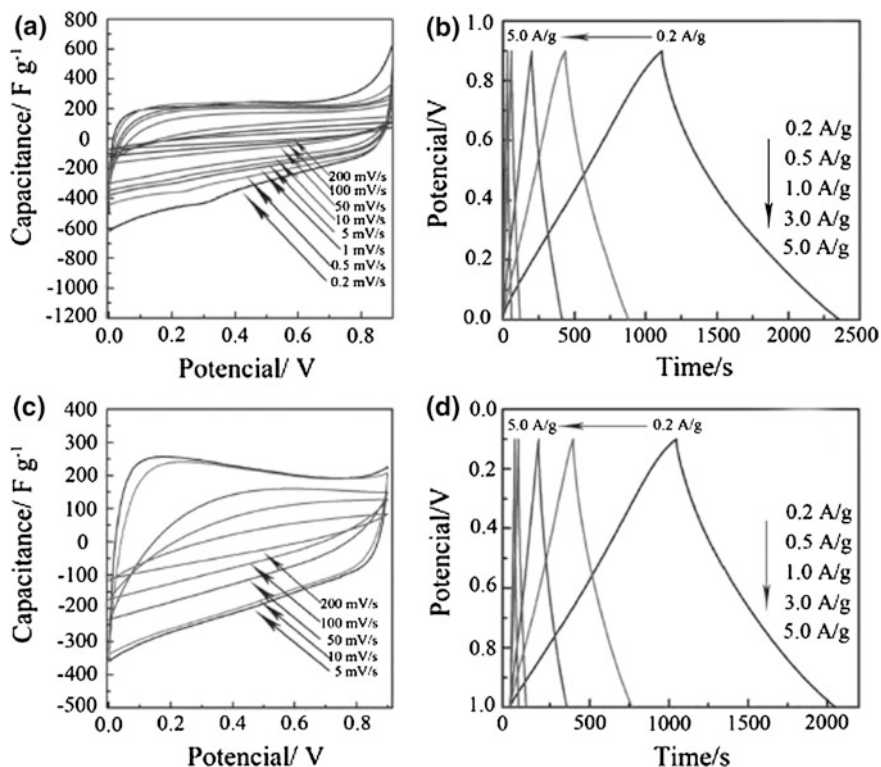


Fig. 11.22 Electrochemical performance of the sample H-NMC-2.5 using a three-electrode cell: cyclic voltammograms at different scan rates in 1 M H₂SO₄ (a) and 6 M KOH (c); and galvanostatic charge/discharge curves at different current densities in 1 M H₂SO₄ (b) and 6 M KOH (d). Reproduced with permission from [3]. Copyright 2013 Wiley-VCH Verlag GmbH & Co. KGaA, Weinheim

11.5 Summary

OMC science has progressed tremendously from the discovery with hard templating strategy in 1999. The ability to control pore sizes that cover all the mesopore range, while maintaining well-defined order motivates research on these materials at the starting time. The recent advances include tuning chemical composition, surface modification, search for sustainable carbon sources or greener synthetic routes. Continued study of OMC material is also focusing on the optimization of volumetric density with high surface area materials, towards high energy storage capacity, because further development of electrochemical capacitors is highly dependent on the development of new electrode materials. The increasing ability to

manipulate the OMC material on nanoscale, including precise control over surface area, pore size, pore structure and surface character, would in principle benefit carbon-based energy applications.

Acknowledgments P.F.Z. and S.D. were supported as part of the Fluid Interface Reactions, Structures, and Transport (FIRST) Center, an Energy Frontier Research Center funded by the U.S. Department of Energy, Office of Science, Office of Basic Energy Sciences.

References

1. M. Antonietti, K. Müllen, Carbon: the sixth element. *Adv. Mater.* **22**, 787 (2010)
2. H. Liang, Q. Guan, L. Chen, Z. Zhu, W. Zhang, S.-H. Yu, Macroscopic-scale template synthesis of robust carbonaceous nanofiber hydrogels and aerogels and their applications. *Angew. Chem. Int. Ed.* **51**, 5101–5105 (2012)
3. J. Wei, D. Zhou, Z. Sun, Y. Deng, Y. Xia, D.Y. Zhao, A controllable synthesis of rich nitrogen-doped ordered mesoporous carbon for CO₂ capture and supercapacitors. *Adv. Funct. Mater.* **23**, 2322–2328 (2013)
4. P.F. Zhang, J. Yuan, T. Fellinger, M. Antonietti, H.R. Li, Y. Wang, Improving hydrothermal carbonization by using poly(ionic liquid)s. *Angew. Chem. Int. Ed.* **52**, 6028–6032 (2013)
5. M. Titirici, M. Antonietti, Chemistry and materials options of sustainable carbon materials made by hydrothermal carbonization. *Chem. Soc. Rev.* **39**, 103–116 (2010)
6. N. Baccile, M. Antonietti, M.-M. Titirici, One-step hydrothermal synthesis of nitrogen-doped nanocarbons: albumine directing the carbonization of glucose. *Chem. Sus. Chem.* **3**, 246–253 (2010)
7. Q. Wang, H. Li, L.Q. Chen, X.J. Huang, Monodispersed hard carbon spherules with uniform nanopores. *Carbon* **39**, 2211–2214 (2001)
8. S. Joo, S. Choi, I. Oh, J. Kwak, Z. Liu, O. Terasaki, R. Ryoo, Ordered nanoporous arrays of carbon supporting high dispersions of platinum nanoparticles. *Nature* **412**, 169 (2001)
9. A.H. Lu, J. Nitz, M. Comotti, C. Weidenthaler, K. Schlichte, C. Lehmann, O. Terasaki, F. Schüth, Spatially and size selective synthesis of Fe-based nanoparticles on ordered mesoporous supports as highly active and stable catalysts for ammonia decomposition. *J. Am. Chem. Soc.* **132**, 14152–14162 (2010)
10. J. Liang, Y. Zheng, J. Chen, J. Liu, D. Hulicova-Jurcakova, M. Jaroniec, S.Z. Qiao, Facile oxygen reduction on a three-dimensionally ordered macroporous graphitic C₃N₄/Carbon composite electrocatalyst. *Angew. Chem. Int. Ed.* **51**, 3892–3896 (2012)
11. Y. Zhai, Y. Dou, D.Y. Zhao, P.F. Fulvio, R.T. Mayes, S. Dai, Carbon materials for chemical capacitive energy storage. *Adv. Mater.* **23**, 4828–4850 (2011)
12. A.B. Fuertes, G. Lota, T.A. Centeno, E. Frackowiak, Templated mesoporous carbons for supercapacitor application. *Electrochim. Acta* **50**, 2799–2805 (2005)
13. H. Liu, X. Wang, W. Cui, Y. Dou, D. Zhao, Y.Y. Xia, Highly ordered mesoporous carbon nanofiber arrays from a crab shell biological template and its application in supercapacitors and fuel cells. *J. Mater. Chem.* **20**, 4223–4230 (2010)
14. Z. Qiao, B. Guo, A.J. Binder, J. Chen, G.M. Veith, S. Dai, Controlled synthesis of mesoporous carbon nanostructures via a “silica-assisted” strategy. *Nano Lett.* **13**, 207–212 (2013)
15. R. Ryoo, S. Joo, S. Jun, Synthesis of highly ordered carbon molecular sieves via template-mediated structural transformation. *J. Phys. Chem. B* **103**, 7743–7746 (1999)
16. J. Lee, S. Yoon, T. Hyeon, S.M. Oh, K.B. Kim, Synthesis of a new mesoporous carbon and its application to electrochemical double-layer capacitors, *Chem. Commun.* **21**, 2177–2178 (1999)

17. Z.J. Li, W.F. Yan, S. Dai, Surface functionalization of ordered mesoporous carbons—a comparative study. *Langmuir* **21**, 11999–12006 (2005)
18. Z.J. Li, S. Dai, Surface functionalization and pore size manipulation for carbons of ordered structure. *Chem. Mater.* **17**, 1717–1721 (2005)
19. S. Jun, S.H. Joo, R. Ryoo, M. Kruk, M. Jaroniec, Z. Liu, T. Ohsuna, O. Terasaki, Synthesis of new, nanoporous carbon with hexagonally ordered mesostructure. *J. Am. Chem. Soc.* **122**, 10712–10713 (2000)
20. H. Darmstadt, C. Roy, S. Kaliaguine, S. Choi, R. Ryoo, Surface chemistry of ordered mesoporous carbons. *Carbon* **40**, 2673–2683 (2002)
21. A.H. Lu, A. Kiefer, W. Schmidt, F. Schüth, Synthesis of polyacrylonitrile-based ordered mesoporous carbon with tunable pore structures. *Chem. Mater.* **16**, 100–103 (2004)
22. Y. Wan, Y. Shi, D.Y. Zhao, Designed synthesis of mesoporous solids via nonionic-surfactant-templating approach. *Chem. Commun.* (9)897–926 (2007)
23. Y. Ren, Z. Ma, P.G. Bruce, Ordered mesoporous metal oxides: synthesis and applications. *Chem. Soc. Rev.* **41**, 4909–4927 (2012)
24. C. Liang, K. Hong, G.A. Guiochon, J.W. Mays, S. Dai, Synthesis of a large-scale highly ordered porous carbon film by self-assembly of block copolymers. *Angew. Chem. Int. Ed.* **43**, 5785–5789 (2004)
25. S. Tanaka, N. Nishiyama, Y. Egashira, K. Ueyama, Synthesis of ordered mesoporous carbons with channel structure from an organic–organic nanocomposite, *Chem. Commun.* 2125–2127 (2005)
26. Y. Wan, Y. Shi, D.Y. Zhao, Supramolecular aggregates as templates: ordered mesoporous polymers and carbons. *Chem. Mater.* **20**, 932–945 (2008)
27. Y. Meng, D. Gu, F. Zhang, Y. Shi, H. Yang, Z. Li, C. Yu, B. Tu, D.Y. Zhao, Ordered mesoporous polymers and homologous carbon frameworks: amphiphilic surfactant templating and direct transformation. *Angew. Chem. Int. Ed.* **44**, 7053–7059 (2005)
28. Y. Deng, T. Yu, Y. Wan, Y. Shi, Y. Meng, D. Gu, L. Zhang, Y. Huang, C. Liu, X. Wu, D.Y. Zhao, Ordered mesoporous silicas and carbons with large accessible pores templated from amphiphilic diblock copolymer poly(ethylene oxide)-b-polystyrene. *J. Am. Chem. Soc.* **129**, 1690–1697 (2007)
29. K.M. Nelson, Z. Qiao, S.M. Mahurin, R.T. Mayes, C.A. Bridges, S. Dai, A non-micellar synthesis of mesoporous carbon via spinodal decomposition. *RSC Adv.* **4**, 23703–23706 (2014)
30. C. Liang, S. Dai, Synthesis of mesoporous carbon materials via enhanced hydrogen-bonding interaction. *J. Am. Chem. Soc.* **128**, 5316–5317 (2006)
31. S. Kubo, R.J. White, N. Yoshizawa, M. Antonietti, M.-M. Titirici, Ordered carbohydrate-derived porous carbons. *Chem. Mater.* **23**, 4882–4885 (2011)
32. S. Schlienger, A. Graff, A. Celzard, J. Parmentier, Direct synthesis of ordered mesoporous polymer and carbon materials by a biosourced precursor. *Green Chem.* **14**, 313–316 (2012)
33. S. Wang, C. Han, J. Wang, J. Deng, M. Zhu, J. Yao, H. Li, Y. Wang, Controlled synthesis of ordered mesoporous carbohydrate-derived carbons with flower-like structure and N-doping by self-transformation. *Chem. Mater.* **26**, 6872–6877 (2014)
34. X. Wang, J. Lee, C. Tsouris, D.W. DePaoli, S. Dai, Preparation of activated mesoporous carbons for electrosorption of ions from aqueous solutions. *J. Mater. Chem.* **20**, 4602–4608 (2010)
35. R. Liu, Y. Shi, Y. Wan, Y. Meng, F. Zhang, D. Gu, Z. Chen, B. Tu, D.Y. Zhao, Triconstituent co-assembly to ordered mesostructured polymer–silica and carbon–silica nanocomposites and large-pore mesoporous carbons with high surface areas. *J. Am. Chem. Soc.* **128**, 11652–11662 (2006)
36. H. Li, R. Liu, D.Y. Zhao, Y.-Y. Xia, Electrochemical properties of an ordered mesoporous carbon prepared by direct tri-constituent co-assembly. *Carbon* **45**, 2628–2635 (2007)